

The deformability of stiff geogrids with interlocked granular material

Z. Rakowski, Consultant, Český Těšín, Czech Republic

J. Kawalec, Tensar International s.r.o., Český Těšín, Czech Republic

L. Horníček, Czech Technical University in Prague, Faculty of Civil Engineering, Prague, Czech Republic

ABSTRACT

Recent concept of mechanically stabilized granular layers is described. The penetration of grains into geogrid apertures results in interlocking phenomenon. By this the grains are immobilized and such part of the layer is stiffened. The deformability of a geogrid plays important role in that mechanism. Results of laboratory experiments where deformation of geogrids with interlocked granular grains were measured are described and evaluated. The data are compared with other data both from laboratory and field observations.

1. INTRODUCTION

Interlocking is already generally accepted mechanism of interaction between stone grains and open structure geosynthetics – geogrids (Cook et al., 2016). Special kind of grains-geogrid composite is formed (Rakowski, Z. 2017). An issue of geogrid deformability is vitally discussed within expert community (Peng et al., 2017, Byun et al., 2019). During experimental works carried out at CTU in Prague (partially published in Horníček, L. et al. 2019) geogrid deformation was measured and evaluated. Detailed results, their interpretation and discussion form the main content of this paper. Results are confronted with a data from some other projects.

2. MECHANICALLY STABILIZED LAYER

Basic mechanism of mechanical stabilization is interlocking of aggregate provided by a geogrid structure (Mahmud et al., 2018, Pires et al., 2018). When granular material is placed and compacted over a geogrid, the aggregate particles penetrate into the apertures and retains against the ribs of the geogrid. This results in locking of the aggregate grain in the aperture under applied load. The stone grain is locked in the aperture when abutting forces are becoming active (Sun et al., 2019). The grain in the next row acts down by contact forces between grains and by that is locked as well. The interlocking is defined as the restriction of the movement of the particles of granular layer under applied load. Shear displacements between grains are very restricted, practically not appearing. The system is stiff and performs almost like “quasi rock” (immobilized grains form a kind of small piece of “massive rock”), see Figure. 1A.

The scheme on Figure 1B shows the principle of layering of mechanically stabilized layer. Within the geogrid and in close vicinity of it the layer is defined as fully confined zone – grain-geogrid composite. Above that is the transition zone which transit into untouched zone is the thickness of the layer is sufficient (Rakowski, Z. 2017).

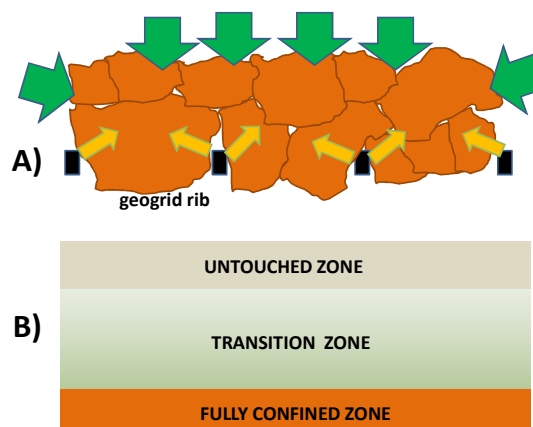


Figure 1. The principle of mechanically stabilized layer.

3. LABORATORY EXPERIMENT

Aforesaid concept of mechanically stabilized layer was verified in experimental box with dimensions of 2.0 x 1.0 x 0.8 m at Czech Technical University in Prague, Faculty of Civil Engineering. The bottom of the experimental box was covered with a thin geotextile for protection of the box. Then the first layer of natural coarse-grained crushed aggregates graded 31.5-63 mm, normally applied for the ballast bed, was laid in a thickness of 150 mm. This layer was adequately compacted with a manual electrical compactor. Backfilling of 100 mm of crushed

gravel graded 31.5-63 mm without compaction followed. The hexagonal geogrid was placed on the levelled layer and was overlaid with a 40 mm thick layer of aggregates and uniformly compacted over the whole surface area. This procedure enabled the necessary aggregate interlocking with the geogrid. Subsequently, another layer of crushed aggregates was laid so that the total layer thickness over the geogrid reached after compaction would be 150 mm. This was followed by backfilling 100 mm of crushed aggregates without compaction and the placement of the second geogrid, the same type as in the first layer. The geogrid was overlaid with a 40 mm thick layer of crushed aggregates, which was uniformly compacted over the whole surface area. Afterwards, the last layer of crushed aggregates was laid with a total thickness of 100 mm over the geogrid after compaction. Longitudinal cross section and top view of the assembled laboratory box are visible on Figure 2, or Figure 3 respectively.

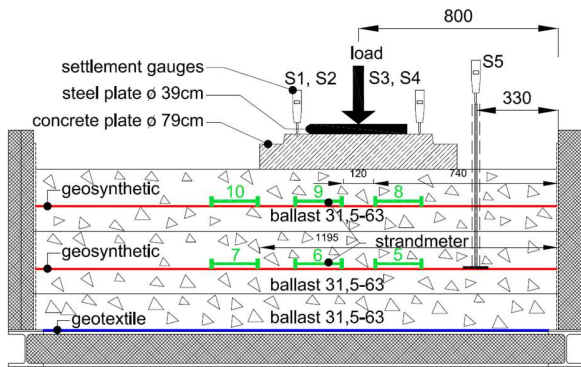


Figure 2. Longitudinal cross section of the experimental box.

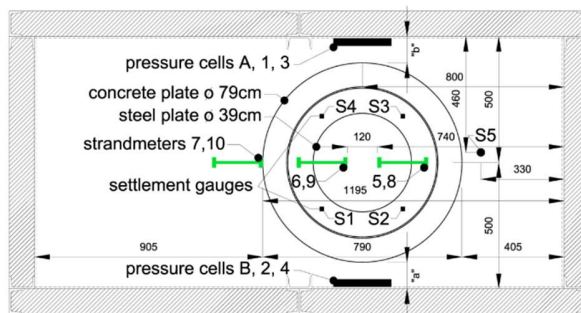


Figure 3. Top view of the experimental box.

During assembly of the construction, three vibrating wire strandmeters of the Geokon 4410 type were mounted along the longitudinal axis of the geogrids at both height levels to allow a precise measurement of the geogrid deformation under loading (see Figure 4). Measurement range of this meters is 3 mm and precision 0.001 mm. The position of strain gauges No. 5-10 along longitudinal axis is shown on Figures 2 and 3. Gauges No. 5, 6, 8, 9 were located under the loading plate by two on upper and lower geogrid. Strain gauges 7 and 10 were located just behind the edge of the plate on lower and upper geogrid respectively. Gauges No. 1-4 were used for other purposes, not treated in this paper. Strandmeters were protected from damage by plastic tubes.

The levelled top layer of aggregate was overlaid with the circular reinforced concrete cover plate, 140 mm in height, 790 mm in diameter and 190 kg in weight, mounted in the position displayed in Figures 2 and 3. On this plate, a circular steel plate, 40 mm in height, 390 mm in diameter and 36 kg in weight was placed. Then the whole construction was exposed to long-term cyclic loading with a force ranging between 3 kN and 100 kN with a sinusoidal course and frequency of 3 Hz. The force was applied in the central position of the upper surface of the circular steel plate by means of the loading hydraulic actuator.

After reaching 1 000, 10 000, 100 000, 200 000, 500 000, 1 000 000, 1 500 000 and 2 000 000 loading cycles, the cyclic loading was interrupted and static loading of the construction with the concrete plate running was applied. The steel plate center was exposed to vertical static loading amounting to 100 kN, corresponding to overall loading with 0.20 MPa under the reinforced concrete plate. The load was applied in 4 steps 25 kN in magnitude, where the concrete plate settlement and strandmeter's values were read 1 minute after the respective loading had been reached (after consolidation). The measurement was carried out in the loading mode of 0-25-50-75-100-0 kN. The settlement was measured by four digital settlement gauges (S1-S4) with an accuracy of 0.01 mm distributed along the concrete plate perimeter. The settlement gauges were fixed onto the concrete plate by means of independently mounted transverse metal frames. Settlement gauge S5 was mounted along the longitudinal axis of the experimental box onto the surface of the first geogrid for the measurement of the geogrid vertical movement under loading. General view of the laboratory set is visible on Figure 5.

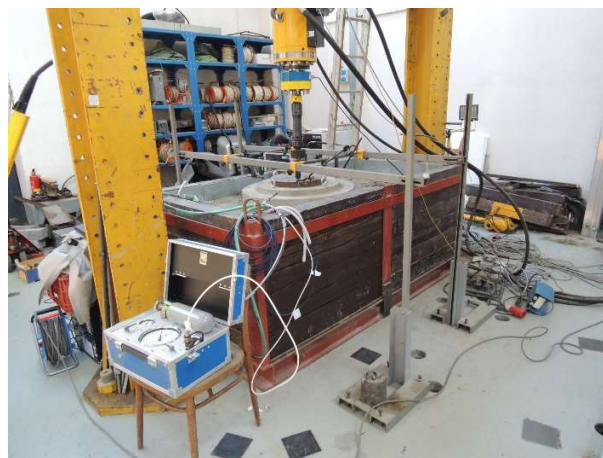


Figure 4. Vibrating wire strain gauge on the geogrid.

Figure 5. General view of the laboratory box.

4. THE DEFORMATION OF THE GEOGRID FROM THE LABORATORY TRIALS

Recorded data by strain gauges are presented on Figures 6-11. Deformations on the graphs are presented in mm. Because they are in various ranges, it is not possible to compare them directly. It requires a bit deeper analysis. All gauges apart of No. 7 and No. 10 recorded the tension, No. 10 records the compression. This is very likely due to its location on the edge of load. No. 7 records are rather chaotic. It seems that grains are relocated every new stage of loading. Also it is the evidence of transition position of the gauge where tension alternates with compression. The values of strain vary in small range. Strains on gauges No. 6, 8 and 10 rapidly grew after first 100 loading cycles, then the strain increment is very small. It means that small relocation of grains within the geogrid aperture in the beginning happened and then they stick practically in the same position. The differences of strain values after loading from 0-100 kN are very small, in cases of the gauges No. 8, 9, 10 practically negligible (apart of gauge No. 7).

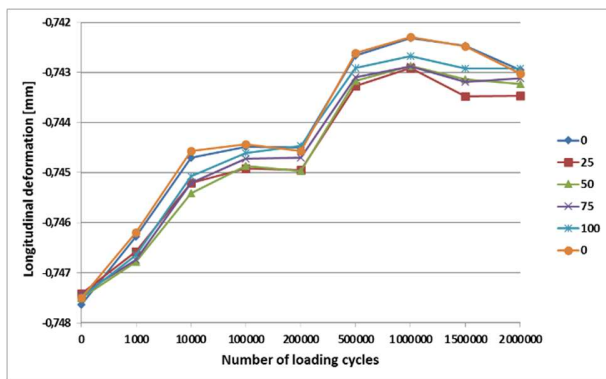


Figure 6. Strain gauge No. 5.

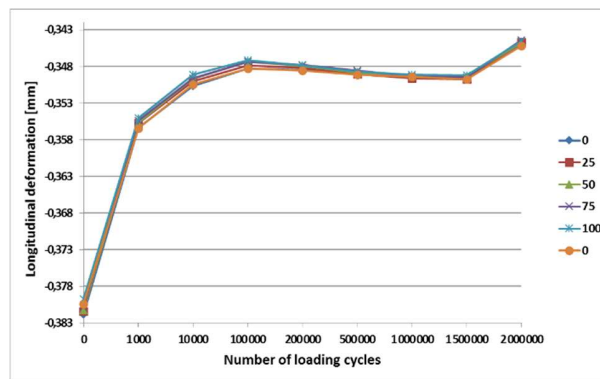


Figure 7. Strain gauge No. 6.

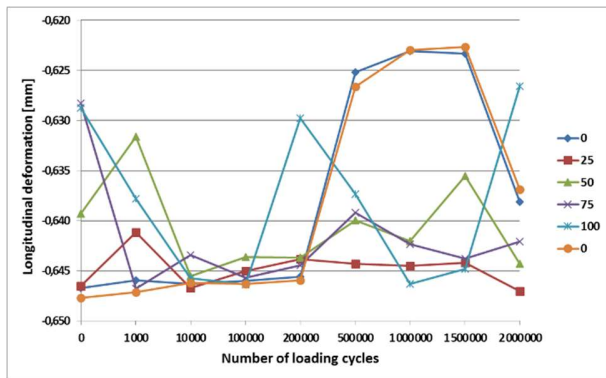


Figure 8. Strain gauge No. 7.

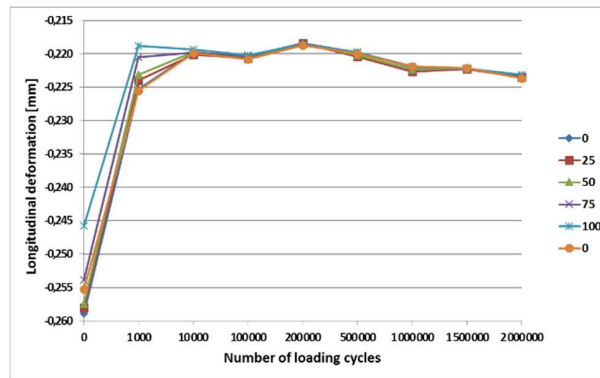


Figure 9. Strain gauge No. 8.

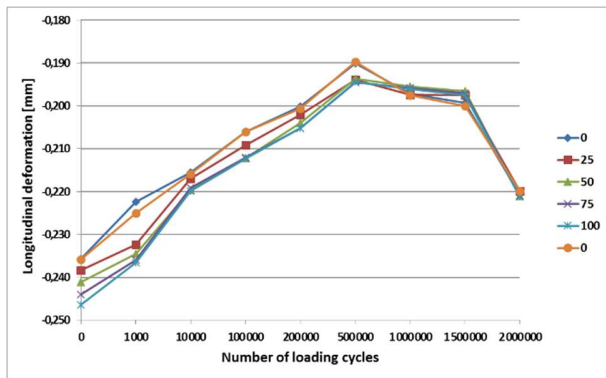


Figure 10. Strain gauge No. 9.

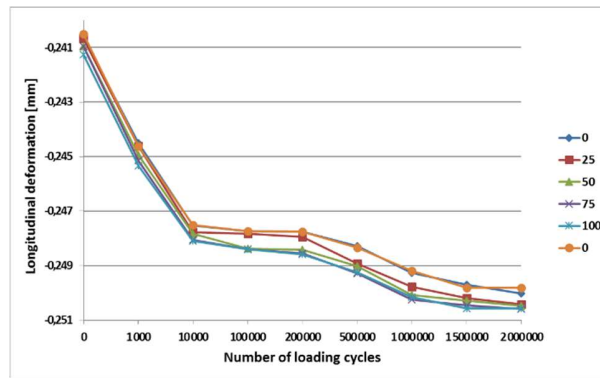


Figure 11. Strain gauge No. 10.

Some generalization has been done to demonstrate the gauges records (apart of No.10) in one graph, see Figure 12. Very small values and range of the strain are in all cases well visible. The range of fluctuation of the gauge No. 7 is shown in the form of grey zone. It means very low deformability of the geogrid once interlocked with stone grains with negligible fluctuation during 2 millions of cycling loading and/or static load of the layer up to 100 kN.

After releasing the load, the permanent strain was recorded at every stage of the experiment, see Figure 13. After some kind of “additional” compaction by cycling loading up to 1k load cycles practically no more permanent strain was recorded. It is very important observation bringing the evidence of the effect of immobilization of the grains and existence of the grain-geogrid composite in the vicinity of the geogrid.

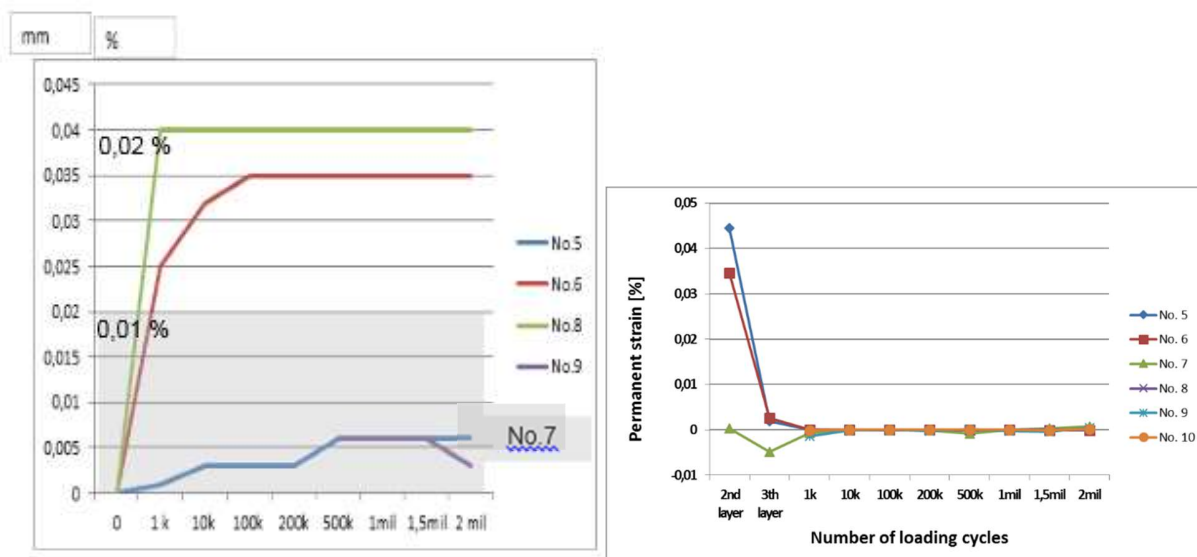


Figure 12. Generalized strain records in common scale. Figure 13. Permanent strain by gauges after releasing the load.

5. SOME RESULTS FROM FIELD TRIALS

Next data were taken from the field trial where the mechanically stabilized layer was loaded by the actuator on special plate counterweighted by heavy crane, see Figure 14. Strain gauges were located on both geogrids. Mechanically stabilized layer was placed over two meters sand pillow over weak soil beneath.

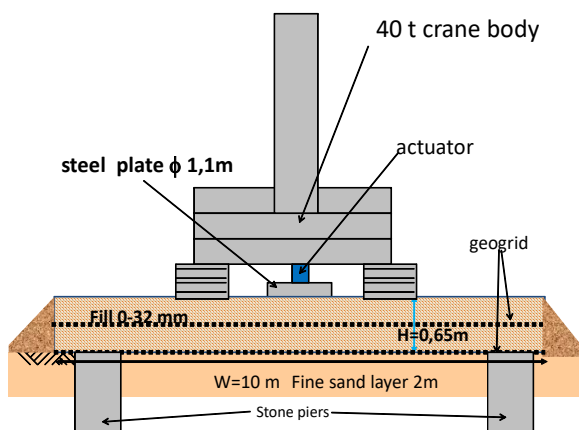
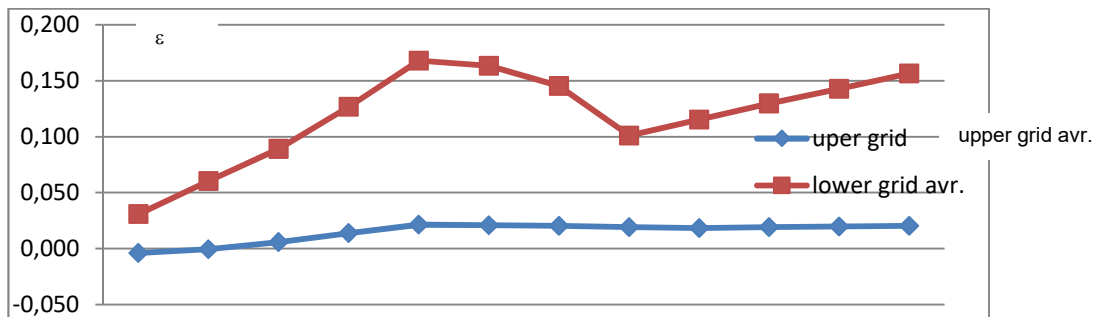


Figure 14. Field trial with heavy crane arrangement.

The record – average from 3 strain gauges located on each geogrid under the loaded plate - is shown on Figure 15. Loading was executed in two cycles, real loads are visible under the graph. The strains in the upper geogrid are very small as it is located in the middle of mechanically stabilized layer. Lower geogrid is located over weaker sand and therefore manifests bigger strains and more distinct reactivity on the changes of the load.



12,04	22,7	33,42	42,52	51,96	29,9	12,25	1,344	12,18	22,32	31,09	31,09	50,74
-------	------	-------	-------	-------	------	-------	-------	-------	-------	-------	-------	-------

8,486	16,18	23,26	29,09	35,54	22,21	9,121	0,876	8,705	15,89	21,79	28,46	34,36
-------	-------	-------	-------	-------	-------	-------	-------	-------	-------	-------	-------	-------

Vertical pressure P [kPa]

Figure 15. Strains in geogrids under the load of the actuator.

Figure 16 shows the further field experiment by Kawalec (Kawalec et al. 2019) where mechanically stabilized layer was installed over extremely weak fill of the power station tail pond covered by shallow water. The mechanically stabilized layer was loaded by 10 rows of concrete slabs. The strain was measured step by step as the loading was increasing. The strain development is seen on Figure 17.

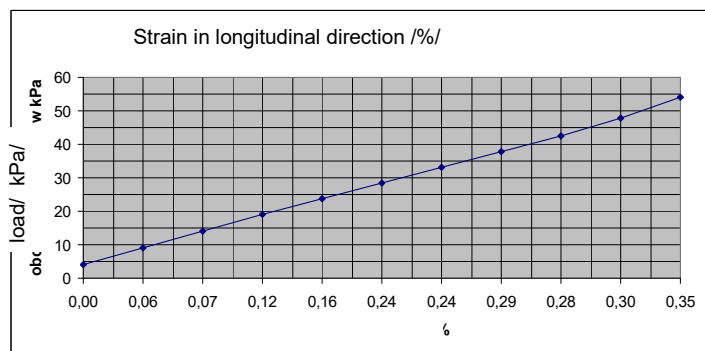


Figure 16. Field trial with 10 rows of slabs over the MSL.

Figure 17. Strain in the geogrid.

6. OBSERVATIONS

From executed laboratory and field trials we can formulate some observations:

- The strains in geogrids are generally very small, both in cyclic and static loading regress.
 - In the trials which were executed strains not exceed 0.35 %.
 - After approx. 1k cycles the system geogrid-soil is fully locked.
 - Permanent strains are practically negligible.
- It means that grains are almost completely immobilized in the geogrid apertures.
 - The strains are dependent on the soil beneath the geogrid.
- The weaker is the soil beneath the geogrid the greater strains were recorded.

7. SUMMARY

Both laboratory and field trials enabled measurement of strains in geogrids. The strains in geogrids are generally very small in range of 0.1 % x n. There is direct relation to the properties of the soils under geogrids. More tests are needed to get some larger statistics.

8. ACKNOWLEDGEMENTS

This study was financially supported by Tensar International, s.r.o. This financial support is gratefully acknowledged.

8.1 REFERENCES

- Byun, Y. H., Tutumluer, E., Feng, B., Kim, J. H., & Wayne, M. H. (2019). Horizontal stiffness evaluation of geogrid-stabilized aggregate using shear wave transducers. *Geotextiles and Geomembranes*, 47(2), 177-186.
- Cook, J., Dobie, M., & Blackman, D. (2016). The development of APT methodology in the application and derivation of geosynthetic benefits in roadway design. In *The Roles of Accelerated Pavement Testing in Pavement Sustainability* (pp. 257-275). Springer, Cham.
- Horníček, L., & Rakowski, Z. (2018). Mechanically Stabilized Granular Layers-An Effective Solution for Tunnel Projects. In *International Congress and Exhibition "Sustainable Civil Infrastructures: Innovative Infrastructure Geotechnology"* (pp. 169-180). Springer, Cham.
- Kawalec, J.; Grygierek, M.; Koda, E.; Osiński, P. Lessons Learned on Geosynthetics Applications in Road Structures in Silesia Mining Region in Poland. *Appl. Sci.* 2019, 9, 1122.
- Mahmud, S. N., Mishra, D., & Potyondy, D. O. (2018). Effect of Geogrid Inclusion on Ballast Resilient Modulus: The Concept of 'Geogrid Gain Factor'. In *2018 Joint Rail Conference* (pp. V001T01A005-V001T01A005). American Society of Mechanical Engineers.
- Sun, X., Han, J., Wayne, M. H., Parsons, R. L., & Kwon, J. (2014). Experimental Study on Resilient Behavior of Triaxial Geogrid-Stabilized Unpaved Roads. In *Ground Improvement and Geosynthetics* (pp. 353-362).
- Peng, X., & Zornberg, J. G. (2017). Evaluation of load transfer in geogrids for base stabilization using transparent soil. *Procedia engineering*, 189, 307-314.
- Pires, D., Barroso, M., Fontul, S., & Dimitrovová, Z. (2018). The study of the interlock of ballast in triaxial geogrids. In *MATEC Web of Conferences* (Vol. 211, p. 12001). EDP Sciences.
- Rakowski, Z. (2017). An attempt of the synthesis of recent knowledge about mechanisms involved in stabilization function of geogrids in infrastructure constructions. *Procedia engineering*, 189, 166-173.